HHS Public Access

Author manuscript

*J Vis Exp*. Author manuscript; available in PMC 2023 July 20.

# Comprehensive Echocardiographic Assessment of Right Ventricle Function in a Rat Model of Pulmonary Arterial Hypertension

**Paola C. Rosas**[*,1], **Liomar A. A. Neves**[*,2], **Peter B. Senese**[2], **Michael R. Gralinski**[2]

[1]Department of Pharmacy Practice, College of Pharmacy, University of Illinois at Chicago

[2]CorDynamics, Inc.

## Abstract

Pulmonary arterial hypertension (PAH) is a progressive disease caused by vasoconstriction and remodeling of the small arteries in the lungs. This remodeling leads to increased pulmonary vascular resistance, worsened right ventricular function, and premature death. Currently approved therapies for PAH largely target pulmonary vasodilator pathways; however, recent emerging therapeutic modalities are focused on other novel pathways involved in the pathogenesis of the disease, including right ventricle (RV) remodeling. Imaging techniques that allow longitudinal assessment of novel therapeutics are very useful for determining the efficacy of new drugs in preclinical studies. Noninvasive trans-thoracic echocardiography remains the standard approach to evaluating heart function and is widely used in rodent models. However, echocardiographic evaluation of the RV can be challenging due to its anatomical position and structure. In addition, standardized guidelines are lacking for echocardiography in preclinical rodent models, making it difficult to carry out a uniform assessment of RV function across studies in different laboratories. In preclinical studies, the monocrotaline (MCT) injury model in rats is widely used to evaluate drug efficacy for treating PAH. This protocol describes the echocardiographic evaluation of the RV in naive and MCT-induced PAH rats.

## Introduction

PAH is a progressive disease defined as a mean pulmonary arterial pressure at rest of greater than 20 mmHg[1]. Pathological changes in PAH include pulmonary artery (PA) remodeling, vasoconstriction, inflammation, and fibroblast activation and proliferation. These pathological changes lead to increased pulmonary vascular resistance and, consequently, right ventricular remodeling, hypertrophy, and failure[2]. PAH is a complex disease that involves crosstalk between several signaling pathways. The currently approved drugs for treating PAH mostly target vasodilator pathways, including the nitric oxide-cyclic guanosine monophosphate pathway, prostacyclin pathway, and endothelin pathway.

**Corresponding Author Liomar A. A. Neves**, neves@cordynamics.com.
*These authors contributed equally

A complete version of this article that includes the video component is available at http://dx.doi.org/10.3791/63775.

Disclosures
The authors have nothing to disclose.

Therapeutics targeting these pathways have been used as both monotherapies and in combination therapies[3,4]. Despite the advances in treatment for PAH in the last decade, findings from the US-based REVEAL registry show a poor 5 year survival rate for newly diagnosed patients[5]. More recently, emerging therapeutic modalities have focused on disease-modifying agents that can impact the multifactorial pathophysiology of the vascular remodeling occurring in PAH in the hope of disrupting the disease[6].

Animal models of PAH are invaluable tools in assessing the efficacy of new drug treatments. The MCT-induced PAH rat model is a widely used animal model characterized by remodeling of the pulmonary arterial vessels, which in turn leads to increased pulmonary vascular resistance and right ventricular hypertrophy and dysfunction[7,8]. To assess the efficacy of new treatments, researchers normally focus on the terminal assessment of RV pressure without considering the longitudinal evaluation of PA pressure, RV morphology, and RV function. The use of noninvasive and non-terminal imaging techniques is crucial for a comprehensive examination of disease progression in animal models. Transthoracic echocardiography remains the standard approach to evaluating heart morphology and function in animal models due to its low cost and ease of use compared to other imaging modalities, such as magnetic resonance imaging. However, echocardiographic evaluation of the RV can be challenging due to the RV positioning beneath the sternum shadow, its well-developed trabeculation, and its anatomical shape, all of which make it difficult to delineate the endocardial border[9,10,11].

This article aims to describe a comprehensive protocol to evaluate RV dimensions, areas and volumes, and systolic and diastolic function in naive and MCT-induced PAH in Sprague Dawley (SD) rats. Additionally, this protocol details a method to assess echocardiographic dimensions in the normal and dilated right atrium.

## Protocol

All experiments in this protocol were performed following the animal care guidelines of the University of Illinois at Chicago, Chicago Institutional Animal Care and Use Committee. Male Sprague Dawley (SD) rats weighed between 0.200-0.240 kg at the time of MCT injection; however, the protocol described in this article can be used with a wider body weight range. The animals were obtained from a commercial source (see Table of Materials).

### 1. Study design

1. Animals
    1. Obtain male SD rats and allow them to acclimate for 4-7 days. Group-house the rats by the experimental group in clean cages and keep them in a room maintained at 20-26 °C (68-79 °F) and illuminated with fluorescent lights timed to give a 14 h light, 10 h dark cycle.
    2. Give rats *ad libitum* access to a standard diet and tap water for the duration of the experiment.

2. MCT administration

    1. On Study Day 0, administer to the rats a subcutaneous dose (3.0 mL/kg) of MCT (60 mg/kg in HCl/NaOH, pH 7.4; see Table of Materials; MCT Group) or vehicle (deionized water, pH 7.4; Control Group).

        NOTE: Due to handling precautions associated with MCT dosing, all rats should be dosed on Study Day 0 in a chemical hazard housing room and housed there until Study Day 7.

    2. On Study Day 7, transfer the rats back to a general housing room for the duration of the study.

3. Clinical observations

    1. Perform cage side observations for general health and appearance once daily. Observe the animals for mortality and signs of pain and distress.

    2. Record any unusual observations noted throughout the duration of the study in the raw data notebook.

4. Body weights

    1. Record body weights on Study Day 0 (predose), weekly throughout the study, and on the day of echocardiography.

## 2. Echocardiography

1. Preparation

    1. On Study Day 23 post-MCT dosing, anesthetize the rats with isoflurane at 2%-3%, driven by 100% oxygen (1 L/min) in an induction chamber (see Table of Materials).

    2. Remove the rats from the chamber once consciousness has been lost and transfer them to the imaging station animal platform (see Table of Materials) in a dorsal decubitus position. Administer isoflurane using a nose cone connected to a vaporizer that delivers 1%-2% isoflurane driven by 100% oxygen (1 L/min).

    3. Apply electrode gel to each paw and secure the paws in the electrocardiogram lead plates of the animal platform.

    4. Remove the fur by shaving the chest and using a depilating agent (see Table of Materials). Secure a rectal temperature probe (see Table of Materials) in place. Place cotton rolls on the animal's right and left sides and secure them with tape to maintain the animal's position when the platform is tilted.

2. Monitoring

    1. Monitor body temperature and heart rate (HR) *via* the ultrasound imaging system (see Table of Materials) throughout the procedure.

2. Keep the body temperature at 37 ± 0.5 °C and maintain the HR at 350 bpm or above, if possible. Use the warming table and a heat lamp to maintain the temperature.

3. Image acquisition

    1. Perform transthoracic echocardiography using a high-frequency ultrasound image system equipped with a solid-state array ultrasound transducer (see Table of Materials).

        NOTE: All directions noted in the echocardiographic methods refer to the right or left of the sonographer.

    2. Left ventricular (LV) parasternal long axis (PLAX) view

        1. With the rats in the dorsal decubitus position, tilt the platform to the left and bring it caudally down approximately 10°.

        2. Place the transducer in the holder in a semilock position with the notch pointing in the caudal direction. Move the transducer so it is pointing toward the left parasternal line. Rotate the transducer counterclockwise approximately 30°-45° and slightly tilt cranially along the y-axis (lateral transducer axis).

        3. Apply warm ultrasound gel (see Table of Materials) to the rat's chest and lower the transducer until it is in contact with the gel.

        4. Move the platform to the right or left to obtain a view of the entire LV in the center of the screen. Adjust the image depth if necessary and move the focal zone to the posterior wall.

        5. Make fine adjustments in the platform position to ensure the aorta and apex are in the same horizontal plane, and the LV outflow tract is visible.

        6. Press **Cine Store** to record the data. Examples of PLAX views of the LV images are shown in Figure 1A.

            NOTE: Imaging the LV allows for familiarity with the position of the heart in the chest. A dilated RV can displace the LV.

    3. Modified PLAX view of the right ventricular outflow tract

        1. Tilt the platform to the right approximately 10°-15° and bring it caudally down approximately 5°.

        2. Move the transducer to point to the right parasternal line of the rat. Rotate the transducer counterclockwise at approximately 30°.

3. Apply ultrasound gel to the rat's chest and lower the transducer until it is in contact with the gel.

4. Move the platform to the left or right until the RV is in view. In this modified PLAX view, the RV wall and interventricular septum (IVS) are clearly visible, as shown in Figure 1B.

5. Rotate the transducer counterclockwise if necessary to ensure the aorta and mitral valve are visible.

6. Move the focal zone to the RV free wall region to improve the endocardial border definition and adjust the gain if necessary.

7. Press **Cine Store** to record the data.

8. Place the M-mode sample volume line at the region where the RV is widest and adjust the gate to encompass the RV and LV. The sample volume line is generally placed between the shadow of two contiguous vertebrae in rats.

9. Press **Update** and then press **Cine Store** to record the data. Examples of M-mode at the modified PLAX view images are shown in Figure 1C, and these images are used to analyze the RV internal diameter during diastole (RVIDd), RV internal diameter during systole (RVIDs), and RV free wall thickness (RVFWT).

10. Lift the transducer and reposition it so it is only slightly inclined toward the right parasternal line of the rat. Move the platform to a position that is only slightly tilted to the right.

11. Lower the transducer until it is in contact with the gel.

12. Move the platform caudally and to the right or left until the RV outflow track is in view and the pulmonary valve (PV) is in focus and clearly visible.

13. Press **Cine Store** to record the data. Examples of B-mode at the modified PLAX view at the level of the right ventricular outflow tract images are shown in Figure 2A; these images are used to analyze the PV diameter.

14. Maintaining the same B-mode image location, press **Color** to aid the identification of flow through the PV. Adjust the velocity to optimize aliasing, so the highest velocity point is visible. Increase the frame rate, if necessary, by decreasing the size of the color Doppler image box.

15. Press **PW** (pulsed wave) to quantify the blood flow spectrum. Increase the sample volume gate size to maximum.

16. Adjust the baseline velocity and the Doppler gain, if necessary, so that the flow is visible.

17. Align the PW angle parallel to the direction of the flow through the PV. Place the sample volume at the highest velocity (point of aliasing) or at the tips of the PV leaflet.

18. Press **Update** to view the pulmonary velocities.

19. Press **Cine Store** to record the data. Examples of PV PW Doppler images are shown in Figure 2B; these images are used to analyze the pulmonary ejection time (PET), pulmonary acceleration time (PAT), pulmonary peak systolic velocity (PV PSV), cardiac output (PV CO), stroke volume (PV SV), HR, and cardiac cycle length (CL).

4. RV focused apical four-chamber view

    1. Tilt the platform to the left corner and down cranially as far as it can go.

    2. Rotate the transducer counterclockwise 30°-45°, and move the transducer so it is pointing to the animal's right shoulder/ear.

    3. Lower the transducer until it is in contact with the gel. This position allows for a typical four-chamber view where the LV and left atria (LA) are visible, but the sternum shadow is over the RV free wall.

    4. Adjust the apical four-chamber view to acquire the RV focused view by placing the transducer slightly lateral to the true apex. Make fine adjustments until the maximal plane is obtained. Move the platform slightly caudally if necessary. In this view, the shadow of the sternum is positioned in the septum, and the RV free wall is clearly visible.

    5. Ensure that the RV, right atria (RA), and tricuspid valve (TV) are visible in the acoustic window.

        NOTE: If the RV chamber is very dilated, the LV chamber may not be completely visible. Holding the transducer manually allows for fine adjustment of the transducer angle to improve RV visualization.

    6. Ensure that the RV is not foreshortened and that the LV outflow tract is not opened up.

    7. Press **Cine Store** to record the data. Examples of B-mode at the RV focused apical four-chamber view images are shown in Figure 3A,B; these images are used to analyze the right atrial area (RAA), RV end-diastolic area (RVEDA), and RV end-systolic area (RVESA).

8. Place the M-mode cursor through the tricuspid annulus at the RV free wall. Ensure to have optimal image orientation to avoid the underestimation of velocities. Press **Update** and **Cine Store** to record the data.

   NOTE: Examples of tricuspid annulus' movement images are shown in Figure 4A,B; these images are used to analyze the tricuspid annular plane systolic excursion (TAPSE).

9. Press **B-Mode** and then press **Color** to aid the identification of flow through the TV. Adjust the velocity to optimize aliasing, so the highest velocity point is visible. Increase the frame rate by decreasing the size of the color Doppler image box.

10. Press **PW** to quantify the blood flow spectrum. Increase the sample volume gate size to maximum.

11. Adjust the baseline velocity and the Doppler gain if necessary.

12. Align the PW angle parallel to the direction of the RV inflow. Place the sample volume at the highest velocity (point of aliasing) or at the tips of the tricuspid leaflet.

    NOTE: Imaging the tricuspid inflow velocities can be challenging; fine adjustment of the transducer position may be necessary.

13. Press **Update** to view the tricuspid inflow velocities.

14. Press **Cine Store** to record the data. Examples of tricuspid PW Doppler images are shown in Figure 5A,B; these images are used to analyze the velocity of blood flow across the TV during early diastolic filling (E), the velocity of blood flow across the TV during late diastolic filling (A), tricuspid closure open time (TCO), and ejection time (ET).

15. Return to B-mode and press **Tissue**. Adjust the platform slightly to ensure the tricuspid annulus is clearly visible, and place the tissue Doppler sample volume gate at the tricuspid annulus at the RV free wall. Increase the sample volume gate to maximum width.

16. Adjust the baseline velocity and the Doppler gain if necessary.

17. Press **Update** to view the tissue Doppler image.

18. Press **Cine Store** to record the data. Examples of tissue Doppler images are shown in Figure 6A,B; these images are used to analyze the tricuspid annular velocity at early diastole (E'), the tricuspid annular velocity at late diastole (A'), and tricuspid annular velocity at systole (S').

NOTE: TAPSE and tissue doppler are always measured at the RV free wall and not at the interventricular septum.

4. Image analysis

    1. Perform image analysis offline using the instrument-compatible software (see Table of Materials).

    2. Avoid areas when inspiration occurs for all measurements and always take at least three measurements for each parameter to be analyzed.

    3. Modified parasternal long-axis view of the right ventricular M-mode

        1. Select an image obtained from the modified parasternal long-axis view of the right ventricular M-mode and analyze the RVIDd (mm), RVIDs (mm), and RVFWT (mm).

        2. Select **Depth** from the generic measurement tools.

        3. Trace the internal diameter of the RV chamber at diastole and systole (Figure 1C) and label the measurements as RVIDd and RVIDs, respectively.

        4. Select the **Depth** tool to measure the thickness of the RV free wall. Align the cursor with the peak of the R wave of the ECG and trace the wall at the end-diastole (Figure 1C). Exclude RV trabeculations and papillary muscle from the RV endocardial border, if present, to accurately measure the RV wall thickness. Also exclude epicardial fat, if present, to avoid erroneously increased measurements.

            NOTE: RV trabeculations and papillary muscle show as discontinued lines that follow the RV wall movement. RVIDd, RVIDs, and RVFWT measurements will be displayed in the report under the generic package section. When there is a significant thickening of the pericardium, the measurement of the RV wall may be difficult; thus, select the area of analysis carefully.

    4. PV B-mode

        1. Select an image obtained from the PV B-mode and analyze the PV diameter (mm).

        2. Select **RV** and **PV Function** from the cardiac package drop-down menu.

        3. Select **PV diam** and choose a frame in which the valve is open. At the level of the valve, trace the distance from wall to wall, avoiding the valve annulus (Figure 2A).

            NOTE: Measurements will be displayed in the report under the RV and PV function section.

5. PV PW Doppler

    1. Select an image obtained from the PV PW Doppler to analyze the PET (ms), PAT (ms), PV PSV (mm/s), HR (beats per min), CL (ms), PAT/PET ratio, cardiac output (PV CO; mL/min), stroke volume (PV SV; μL), and PAT/CL ratio.

    2. Select **RV** and **PV Function** from the cardiac package drop-down menu and choose at least three representative PA velocities.

    3. Select **PAT** and trace the PA flow velocity starting at the point of acceleration and ending at the peak of velocity.

    4. Select **PET** and begin the measurement from the point of acceleration and end when the signal reaches baseline.

    5. Select **PV peak vel**, place the cursor at the highest velocity point, and left click.

    6. To obtain the PV velocity time integral (PV VTI) measurement, choose the negative option under the peak Vevo tool.

        NOTE: The detection sensitivity can be changed, but a constant value should be maintained throughout the study.

    7. Select **PV VTI** from the drop-down menu. Start the measurement by left clicking on the start of the peak and end by right clicking at the end of the peak to complete the measurement. Adjust the peak outline by moving the lines as necessary.

    8. Place the cursor at a PV VTI measurement and right click to select **Properties**, then enable HR measurement in the parameters option. Repeat this step for all three PV VTI measurements.

    9. Select **Time** from the generic measurement tools and trace the time from the point of acceleration of one cycle to the point of acceleration of the next cycle to calculate the CL (Figure 2B).

        NOTE: Measurements will be displayed in the report under the RV and PV function section. PAT/PET ratio, PV CO, and PV SV are calculated by the instrument software.

6. RV focused apical four-chamber view B-mode

    1. Select an image obtained from the RV focused apical four-chamber view B-mode to analyze the RAA ($mm^2$), RVEDA ($mm^2$), RVESA ($mm^2$), and RV fractional area change [RVFAC = (RVEDA-RVESA)/RVEDA, %].

2. Select **SAX** (parasternal short axis) from the cardiac package drop-down menu.

3. Choose a B-mode image at end-diastole from the RV focused apical four-chamber view. Ensure that the entire RV is in the view, including the apex and the lateral wall.

4. Select **ENDOarea;d** and trace the RV endocardium from the annulus, along the free wall to the apex, and then back to the annulus along the interventricular septum, excluding trabeculations if they are present.

5. Choose a B-mode image at end-systole, select **ENDOarea;s** from the SAX B-mode drop-down window, and repeat the trace of the RV. Using the same image, select the **2D area** from the generic measurement tools and trace the RA by following the endocardium and excluding the vena cava and RA appendage. The area between the tricuspid valve leaflets and the annulus is also excluded (Figure 3).

6. Repeat the ENDO area measurement at diastole and systole and RA area measurement in two additional images.

   NOTE: Measurements of the RV area at diastole and systole will be displayed in the report under the SAX-B mode section. RA area will be displayed under the generic package measurements. RVFAC is calculated using the formula RVFAC = (RVEDA-RVESA)/RVEDA[10].

7. M-mode at the lateral part of the tricuspid annulus

   1. Select an M-mode image obtained from the lateral part of the tricuspid annulus to analyze the TAPSE (mm).

   2. Select **Depth** from the generic measurement tools and choose a region of at least three consecutive cardiac sites free of inspiratory interferences.

   3. Trace the distance from end-diastole to peak systole of the RV annular segment in three consecutive cardiac cycles (Figure 4).

      NOTE: Measurements will be displayed in the report under the generic package section.

8. TV PW Doppler

   1. Select an image obtained from the TV PW doppler to analyze the E (mm/s), A (mm/s), TCO (ms), ET (ms), and RV myocardial performance index [RVMPI = (TCO-ET)/ET][11].

   2. Select **TV Flow** from the cardiac package drop-down menu and choose at least three representative TV velocities.

3. Select **TV E** (tricuspid early filling), place the cursor at the highest velocity point of the E wave, and left click; a line is drawn from the highest velocity to the baseline. Similarly, select **TV A** (tricuspid late filling), place the cursor at the highest velocity of the A wave, and left click; another line is drawn from the highest velocity to the baseline (Figure 5).

4. To measure the ejection time (ET), select the **Time** tool from the generic measurement tools and measure the time from the onset (leading edge) to the cessation (trailing edge) of tricuspid inflow (an area where the flow ejects). Label the measurements as ET (Figure 5).

5. To measure the TCO time, select the **Time** tool and trace the time from the end of the tricuspid A wave of one cycle to the beginning of the tricuspid E wave of the next cycle. Label the measurements as TCO (Figure 5).

   NOTE: Measurements of TV E and TV A will be displayed in the report under the TV Flow section. ET and TCO measurements will be displayed under the generic package measurements. RVMPI is calculated as (TCO-ET)/ET11. E, ET, and TCO are measured with a constant R-R interval to minimize error. ET measurements can also be performed from the middle edge to the trailing edge; consistency in how the measurement is acquired throughout analysis is most important.

**9.** RV lateral tricuspid annulus tissue Doppler

1. Select an image obtained from the RV lateral tricuspid annulus tissue Doppler to analyze the E' (mm/s), A' (mm/s), S' (mm/s), and E/E' Ratio.

2. Select **TV Flow** from the cardiac package drop-down menu and choose at least three representative free wall tissue velocities.

3. Select **TV LW E**, place the cursor at the highest velocity point of the E' wave, and left click; a line is drawn from the highest velocity to the baseline. Similarly, select **TV LW A**, place the cursor at the highest velocity point of the A' wave, and left click; another line is drawn from the highest velocity to the baseline (Figure 6).

4. Select **MV Flow** from the cardiac package drop-down menu and select **S WAVE**.

5. Place the cursor at the highest systolic velocity during the ejection phase, without over gaining the Doppler envelope,

and left click; a line is drawn from the highest velocity to the baseline (Figure 6).

NOTE: Measurements will be displayed in the report under the TV Flow and MV Flow sections. The E/E' ratio is calculated manually.

5. Necropsy

1. Euthanize the rats by exsanguination under isoflurane overdose on Study Day 24 post-MCT dosing following institutionally approved protocol.
2. Remove the heart-lung block and gently infuse *via* the vasculature with ice-cold saline until the perfusate runs clear. Separate the heart and lungs and remove the excess saline.
3. Weigh each organ separately.
4. Remove the atria and discard.
5. Separate the LV with the septum (LV+S) from the RV and weigh the ventricles separately.
6. Remove the left tibia and separate it from the soft tissue.
7. Obtain a longitudinal measurement of the tibia using a digital caliper (see Table of Materials).
8. Dispose of the dissected heart, lungs, and tibia with the rest of the carcass.

NOTE: The heart weight (HW), lung weight (LW), LV+S weight, and RV weight are normalized by the tibia length (TL). TheRV hypertrophy is assessed by Fulton's Index, where the RV weight is normalized by the LV+S weight [Fulton index = RV/(LV+S)][12].

## Representative Results

In this study, MCT-treated rats were used as a model of PAH. Echocardiographic analysis was performed on Study Day 23 post-MCT administration, and all measurements and calculations represented averages from three consecutive cycles. Echocardiographic parameters obtained from control (vehicle: deionized water) and MCT-treated (60 mg/kg) rats are shown in Table 1.

Representative images of the PLAX view in control and MCT-treated rats are shown in Figure 1A. These images are used as an initial assessment of the position of the heart and LV morphology. Quantitative assessments of the RV are obtained in a modified PLAX view, because this allows visualization of the RV (Figure 1B). In the modified PLAX view, the MCT-treated rats show an enlarged right ventricle and the left ventricle appears displaced from its position when compared with the control rats (Figure 1B). M-mode is obtained in the modified PLAX view at the widest area of the RV and used to measure RVIDd,

RVIDs, and RVFWT (Figure 1C). RVIDd, RVIDs, and RVFWT are measured, excluding trabeculation in the wall, and RVFWT is obtained at the peak of the R wave of the ECG. As expected, a significant increase in RVIDd, RVIDs, and RVFWT are observed in the MCT-treated rats (Figure 1C and Table 1), indicating RV dilation and thickening of the RV free wall.

Doppler imaging is used to measure PA flow velocities (Figure 2B). In control rats, pulmonary flow exhibits a symmetrical V shape, with a peak velocity that occurs in mid systole (Figure 2B, upper panel). In contrast, in MCT-treated rats, peak velocity is slower and happens earlier in systole, resulting in a significantly shortened PAT and smaller PAT/PET and PAT/CL ratios (Table 1). Additionally, MCT-treated rats exhibit a notch in late systole (Figure 2B, lower panel). PV PW Doppler is used to measure the PV VTI (Figure 2B); PV CO and PV SV are calculated using the PV VTI and PV diameter measurements, respectively. PV CO and PV SV are significantly lower in the MCT-treated rats (Table 1), indicating impaired systolic function. HR is obtained from the PV PW Doppler measurements and is comparable between the control and MCT-treated rats (Table 1).

The RV focused apical four-chamber view is used to measure RVEDA, RVESA, and RAA (Figure 3), and RVFAC is calculated from RVEDA and RVESA. As stated earlier, trabeculations in the wall, if present, must be excluded from these measurements. RVFAC is significantly decreased in MCT-treated rats (Table 1), suggesting RV systolic dysfunction. MCT-treated rats also exhibit RA dilation because of increased PA pressure (Figure 3A,B, right panels, and Table 1). In normal conditions, the LV cavity has a higher pressure than the RV, resulting in a septal curvature of the LV throughout the cardiac cycle (Figure 3A,B, left panels). When the RV pressure pathologically increases in PAH, this normal curvature is lost, and the interventricular septum appears "flattened"[13], as shown in Figure 3A,B (right panels). The RV focused apical four-chamber view is also used to measure TAPSE from the M-mode interrogation of the tricuspid annulus (Figure 4). TAPSE is significantly reduced in MCT-treated rats (Figure 4B and Table 1), suggesting compromised RV function.

Diastolic function is assessed from the PW Doppler evaluation of the TV flow and lateral TV lateral annulus tissue Doppler. MCT-treated rats show a significantly higher E wave and RVMPI and a tendency toward an increased E/E' ratio (Figure 5 and Table 1), suggestive of impaired diastolic function. The TV annulus tissue Doppler view is also used to measure E' and S' (Figure 6B). MCT-treated rats exhibit significantly slower S', confirming decreased RV systolic function (also demonstrated by a reduction in PV CO and PV SV). No significant change in E' is observed in MCT-treated rats. A and A' can also be obtained from the TV flow PW Doppler and lateral TV lateral annulus tissue Doppler, respectively. These parameters are not discussed in this article.

Cardiac tissue mass measurements at terminal harvest and echocardiographic analyses support RV hypertrophy in MCT-treated rats when compared to control rats. As shown in Table 2, Fulton Index and the RV/TL ratio are significantly increased in MCT-treated rats as compared to control rats. Additionally, MCT-treated rats show an increased LV+S/TL

ratio, indicating LV hypertrophy. MCT-treated rats also exhibit an increased LW/TL ratio, suggesting pulmonary edema.

## Discussion

Echocardiographic evaluation of the RV is a valuable discovery tool for the screening of the effectiveness of novel treatments in animal models of PAH. In-depth characterization of the RV structure and function is necessary as novel targets in treating PAH address RV remodeling[4, 14]. This study describes a detailed protocol that allows for the successful characterization of RV structure and function.

The complex structural geometry and positioning behind the sternum make echocardiographic characterization of the RV difficult; thus, modified echocardiographic views are used to facilitate RV visualization and to assist in precise identification of the RV endocardial borders during analyses. In this regard, modified PLAX is used for better visualization and to obtain the pulmonary flow velocities and morphological measurements of the RV. Other protocols have described the use of parasternal short-axis views to measure pulmonary flow and RV wall thickness[15]; however, the use of modified PLAX allows consistent representative views of the pulmonary flow velocities to be obtained, and also improves the RV free wall definition. Additionally, the RV focused four-chamber apical view is used to improve the visualization of the RA and RV chamber walls and consistently obtain measurements of the RV systolic and diastolic parameters.

The following parameters are recommended to assess RV systolic function: TAPSE, RVFAC, RIMP, and S'. TAPSE is a measurement of RV longitudinal contraction and has been reported to correlate with the degree of RV dysfunction[16]; however, TAPSE only evaluates longitudinal contraction without taking into consideration the radial component of contraction that becomes relevant in a dilated RV[11]. Despite its limitation, TAPSE remains a routinely obtained parameter, as it is easier to acquire compared to RVFAC and RIMP; however, a full evaluation of the degree of systolic dysfunction should include the assessment of S', RIMP, and RVFAC. S' is easily measured, reliable, and reproducible, however it only evaluates longitudinal systolic function. In humans, RVFAC correlates well with RV ejection fraction (EF)[10] and is a more accurate measurement of RV function than TAPSE. RIMP, defined as [TCO-ET]/ET, is an index of global RV performance, reflects both RV systolic and diastolic function, and is a prognostic marker in patients with PAH[17]. RIMP is measured from TV PW Doppler since it can be more easily obtained, although it can also be measured from the tissue Doppler of lateral tricuspid annulus. It is important to use several indices of RV systolic function when assessing the effectiveness of drug treatment in PAH animal models to overcome the limitation of each measurement. The use of the RVEF as a measurement of systolic function is not recommended due to the complexity of the RV geometry, which leads to grossly underestimated volumes[10].

RV diastolic function in rats is an understudied area due to the technical difficulties in obtaining the TV flow velocities and the TV lateral annulus tissue Doppler. By using the RV focused four-chamber apical view as stated in this protocol, consistent echocardiographic views with good endocardial border definition can be obtained. E/E' ratio and RAA should

be used as a measure of RV diastolic function in early RV dysfunction. Strain analysis has become a powerful tool to access LV systolic dysfunction at the initial stages of LV dysfunction; however, only a few studies use this type of analysis to evaluate the RV[14, 18], due to the difficulties encountered in visualizing the entire wall and in obtaining high-quality echocardiographic images that are necessary for strain analysis. Although strain analyses were not performed in this study, the quality of the images obtained following this protocol is sufficient to perform this type of analysis, if needed.

Finally, this protocol provides a detailed description of the echocardiographic views necessary to assess RV and RA morphology, as well as to characterize RV systolic and diastolic function. These data provide an enhanced evaluation of the efficacy of novel compounds to disrupt PAH development in rodent animal models.

## Acknowledgments

This work was supported by NHLBI K01 HL155241 and AHA CDA849387 awarded to the author P.C.R.

## References

1. Galie N, McLaughlin VV, Rubin LJ, Simonneau G An overview of the 6th World Symposium on Pulmonary Hypertension. European Respiratory Journal. 53 (1), 1802148 (2019). [PubMed: 30552088]
2. Tyagi S, Batra V Novel therapeutic approaches of pulmonary arterial hypertension. International Journal of Angiology. 28 (2), 112–117 (2019).
3. Hoeper MM et al. Targeted therapy of pulmonary arterial hypertension: Updated recommendations from the Cologne Consensus Conference 2018. International Journal of Cardiology. 272, 37–45 (2018).
4. Sommer N et al. Current and future treatments of pulmonary arterial hypertension. British Journal of Pharmacology. 178 (1), 6–30 (2021). [PubMed: 32034759]
5. Farber HW et al. Five-year outcomes of patients enrolled in the REVEAL registry. Chest. 148 (4), 1043–1054 (2015). [PubMed: 26066077]
6. Zolty R Novel experimental therapies for treatment of pulmonary arterial hypertension. Journal of Experimental Pharmacology. 13, 817–857 (2021). [PubMed: 34429666]
7. Jasmin JF, Lucas M, Cernacek P, Dupuis J Effectiveness of a nonselective ET(A/B) and a selective ET(A) antagonist in rats with monocrotaline-induced pulmonary hypertension. Circulation. 103 (2), 314–318 (2001). [PubMed: 11208695]
8. Stenmark KR, Meyrick B, Galie N, Mooi WJ, McMurtry IF Animal models of pulmonary arterial hypertension: the hope for etiological discovery and pharmacological cure. American Journal of Physiology Lung Cellular and Molecular Physiology. 297 (6), L1013–1032 (2009). [PubMed: 19748998]
9. Muresian H The clinical anatomy of the right ventricle. Clinical Anatomy. 29 (3), 380–398 (2016). [PubMed: 25393337]
10. Rudski LG et al. Guidelines for the echocardiographic assessment of the right heart in adults: a report from the American Society of Echocardiography endorsed by the European Association of Echocardiography, a registered branch of the European Society of Cardiology, and the Canadian Society of Echocardiography. Journal of the American Society of Echocardiography. 23 (7), 685–713 (2010). [PubMed: 20620859]
11. Jones N, Burns AT, Prior DL Echocardiographic assessment of the right ventricle-state of the art. Heart Lung and Circulation. 28 (9), 1339–1350 (2019).
12. Spyropoulos F et al. Echocardiographic markers of pulmonary hemodynamics and right ventricular hypertrophy in rat models of pulmonary hypertension. Pulmonary Circulation. 10 (2), 2045894020910976 (2020). [PubMed: 32537128]

13. Armstrong WF, Ryan T, Feigenbaum H Feigenbaum's echocardiography. 7th edn. Wolters Kluwer Health/Lippincott Williams & Wilkins. (2010).

14. Kimura K et al. Evaluation of right ventricle by speckle tracking and conventional echocardiography in rats with right ventricular heart failure. International Heart Journal. 56 (3), 349–353 (2015). [PubMed: 25912902]

15. Cheng HW et al. Assessment of right ventricular structure and function in mouse model of pulmonary artery constriction by transthoracic echocardiography. Journal of Visualized Experiments. 84, e51041 (2014).

16. Mazurek JA, Vaidya A, Mathai SC, Roberts JD, Forfia PR Follow-up tricuspid annular plane systolic excursion predicts survival in pulmonary arterial hypertension. Pulmonary Circulation. 7 (2), 361–371 (2017). [PubMed: 28597759]

17. Grapsa J et al. Echocardiographic and hemodynamic predictors of survival in precapillary pulmonary hypertension: seven-year follow-up. Circulation: Cardiovascular Imaging. 8 (6), e002107 (2015). [PubMed: 26063743]

18. Bernardo I, Wong J, Wlodek ME, Vlahos R, Soeding P Evaluation of right heart function in a rat model using modified echocardiographic views. PLoS One. 12 (10), e0187345 (2017). [PubMed: 29088272]

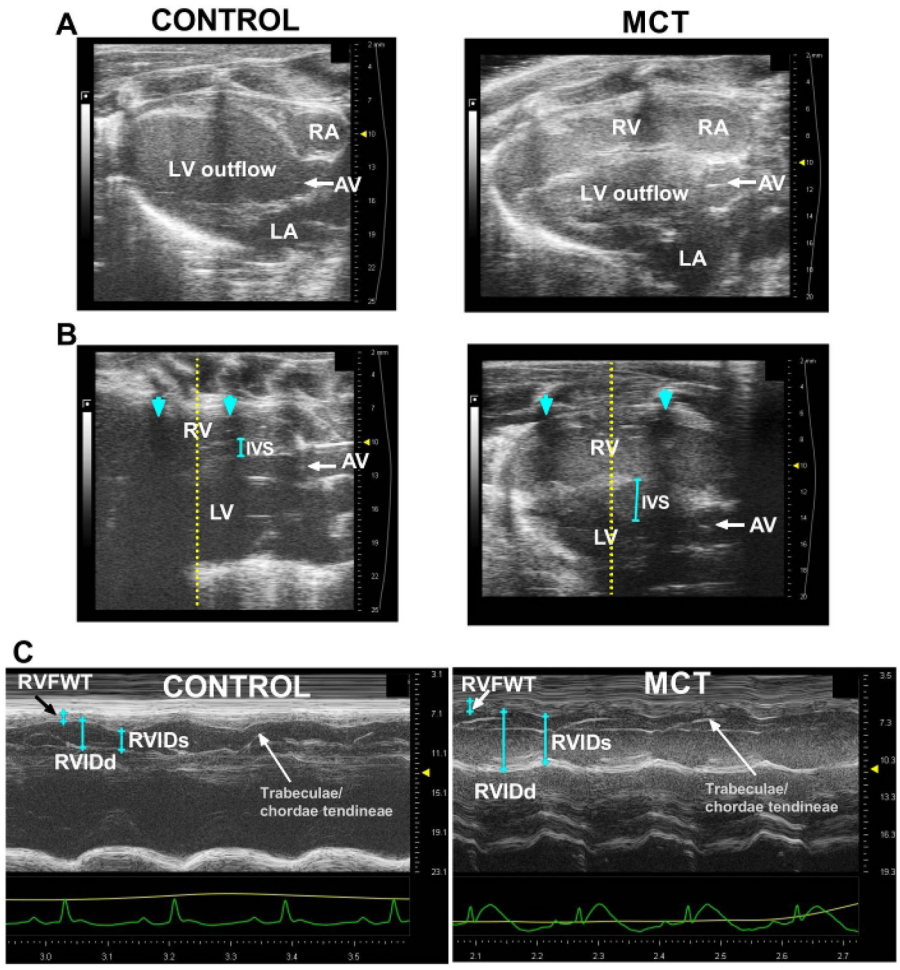


**Figure 1: Parasternal long-axis (PLAX) views.**

(**A**) Representative images of conventional PLAX to visualize the left ventricular (LV) outflow, left atria (LA), right atria (RA), and aortic valve (AV) in a control rat (left panel) and monocrotaline (MCT)-treated rat (right panel). (**B**) Representative images of modified PLAX view to visualize the right ventricular (RV) outflow tract, the interventricular septum (IVS), the LV, and the AV in a control rat (left panel) and MCT-treated rat (right panel). In rats, the M-mode sample volume line is usually placed between the shadow of two contiguous vertebrae (shown with blue arrows). (**C**) Examples of M-mode measurements in a control rat (top panel) and MCT-treated rat (bottom panel). Measurements include RV free wall thickness (RVFWT), RV internal diameter during diastole (RVIDd), and RV internal diameter during systole (RVIDs). For easy viewing, the measurements of only one cardiac cycle are shown.

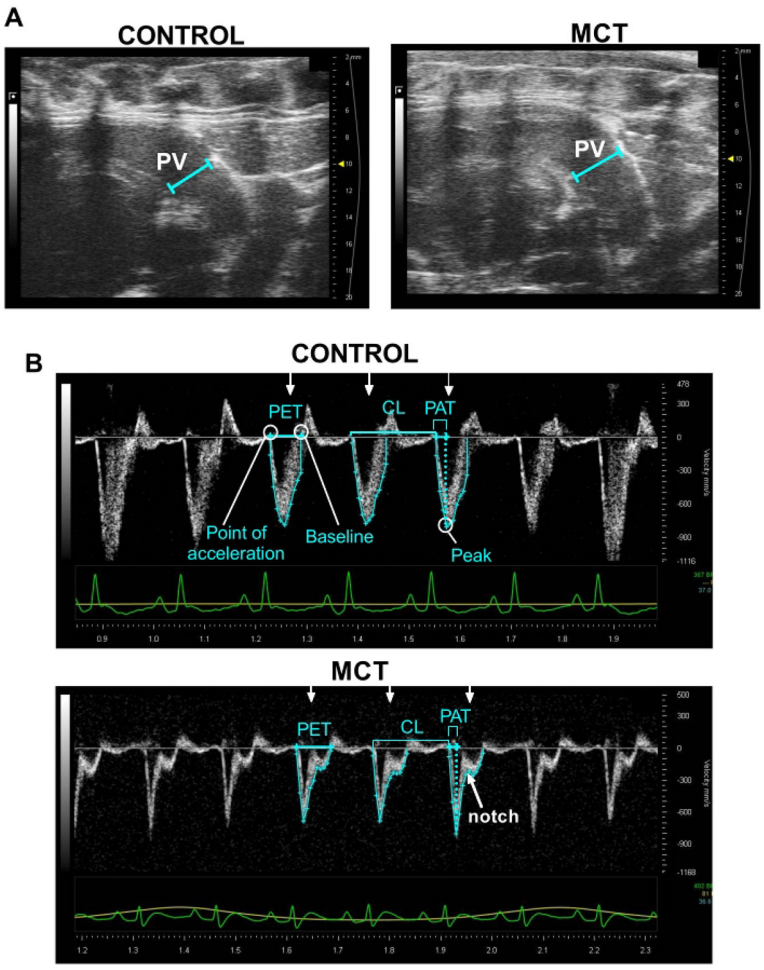


**Figure 2: PV diameter and pulmonary artery flow velocities.**

(**A**) Representative images of modified PLAX view to visualize the pulmonary artery and to measure the pulmonary valve (PV) diameter in a control rat (left panel) and monocrotaline (MCT)-treated rat (right panel). (**B**) Pulmonary ejection time (PET) is measured starting at the point of acceleration to the point of return to baseline in a control rat (top panel) and MCT-treated rat (bottom panel). Pulmonary acceleration time (PAT) is the time interval between the point of acceleration to the peak of velocity. Pulmonary valve peak systolic velocity (PV PSV) is measured at the peak of the Doppler flow. PV velocity time integral (PV VTI) is traced in blue using the software option. Cardiac cycle length (CL) is measured from the point of acceleration of one cycle to the point of acceleration of the next cycle. Late systole notching is observed in MCT-treated rats. Arrows indicate the three consecutive cycles that were considered for calculations. Representative measurements are shown in different cycles for easy viewing, but all measurements were taken in each of the three cycles.

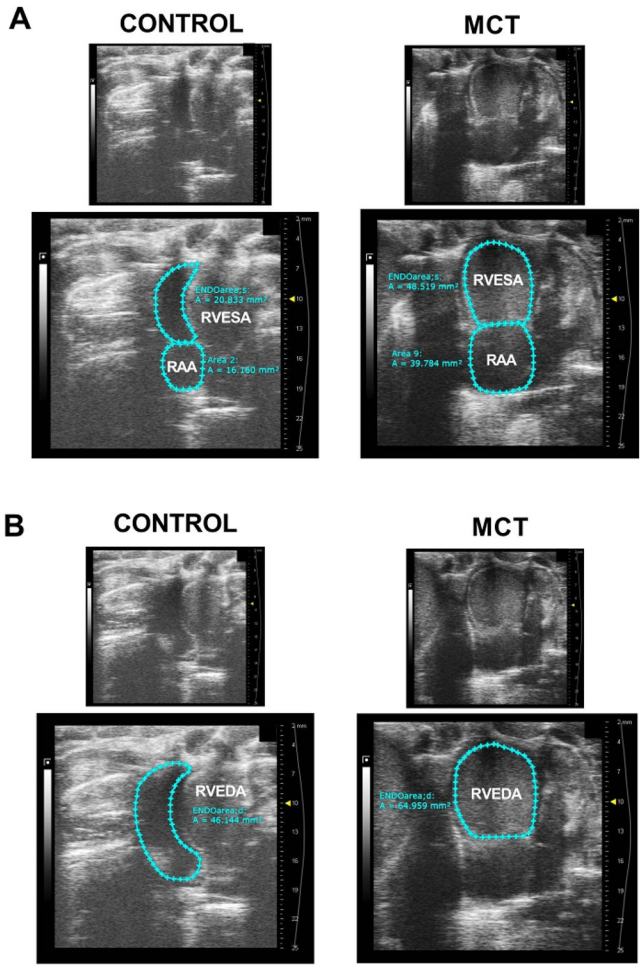


**Figure 3: RV focused apical four-chamber view.**

(**A**) Representative images of the right ventricular end-systolic area (RVESA) and right atrial area (RAA) in a control rat (left panel) and monocrotaline (MCT)-treated rat (right panel). Upper panels show images without tracing, and lower panels show traced areas. Measurements were taken using ENDOarea;s and 2D area tools to calculate RVESA and RAA, respectively. (**B**) Sample images of right ventricle end-diastolic area (RVEDA) using the ENDOarea;d software tool in a control rat (left panel) and MCT-treated rat (right panel). Upper panels show images without tracing, and lower panels show traced areas.

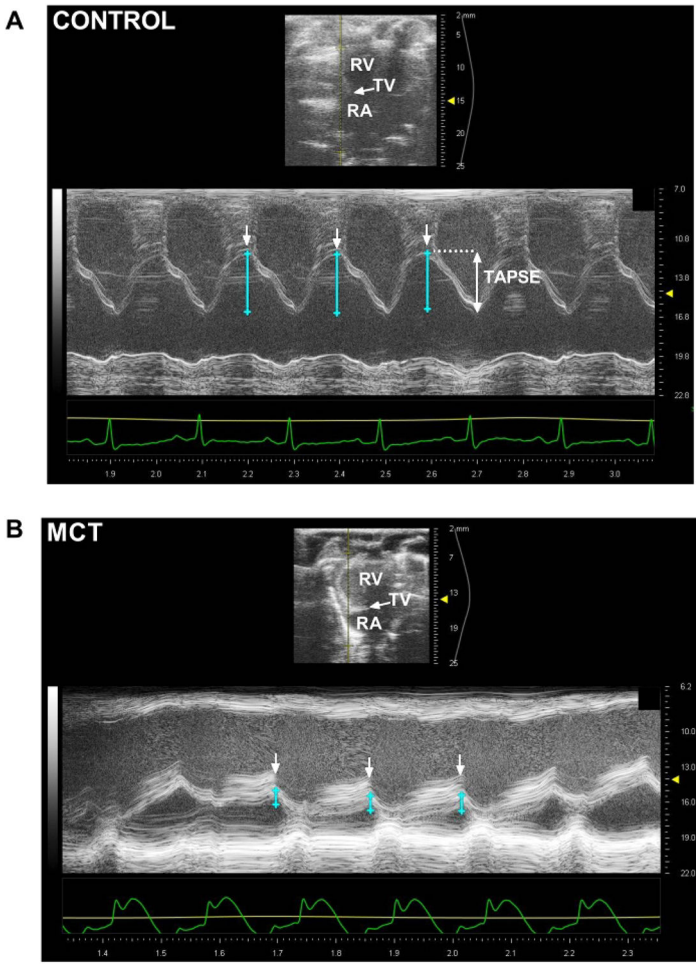


**Figure 4: Tricuspid annular plane systolic excursion (TAPSE).**

(**A**) Upper panel: right ventricular focused apical four-chamber view in a control rat. Right ventricle (RV), right atria (RA), and tricuspid valve (TV) are visualized. Lower panel: M-mode interrogation of the tricuspid annulus to measure TAPSE in control rats. (**B**) Upper panel: right ventricular focused apical four-chamber view in a monocrotaline (MCT)-treated rat. Lower panel: M-mode interrogation of the tricuspid annulus to measure TAPSE in an MCT-treated rat. Arrows indicate the three consecutive measurements that were considered for calculations.

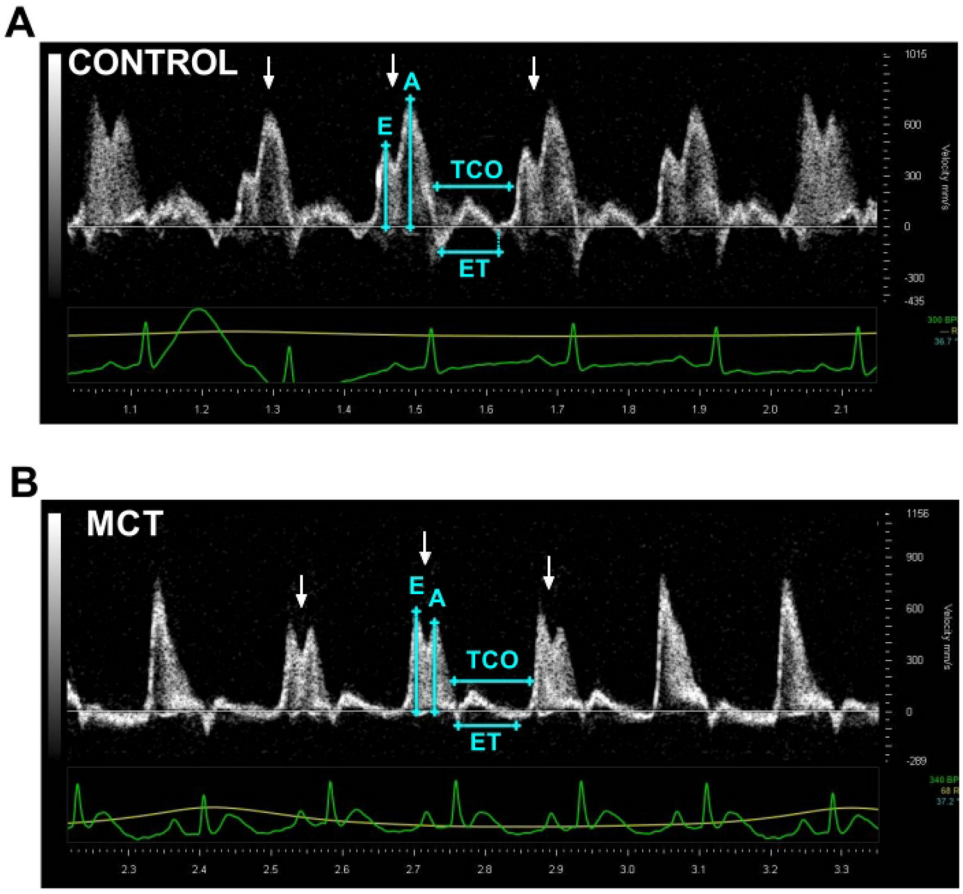


**Figure 5: Pulsed wave Doppler of tricuspid inflow.**

Example of pulsed Doppler recordings of tricuspid inflow to measure the blood inflow velocity across the tricuspid valve during early diastolic filling (E, in blue), late diastolic filling (A, in blue), tricuspid closure-open time (TCO), and ejection time (ET) in (**A**) a control rat and in (**B**) a monocrotaline (MCT)-treated rat. Arrows indicate the three consecutive cycles that were considered for calculations. Representative measurements are shown in one cycle for easy viewing, but all measurements were taken in each of the three cycles.

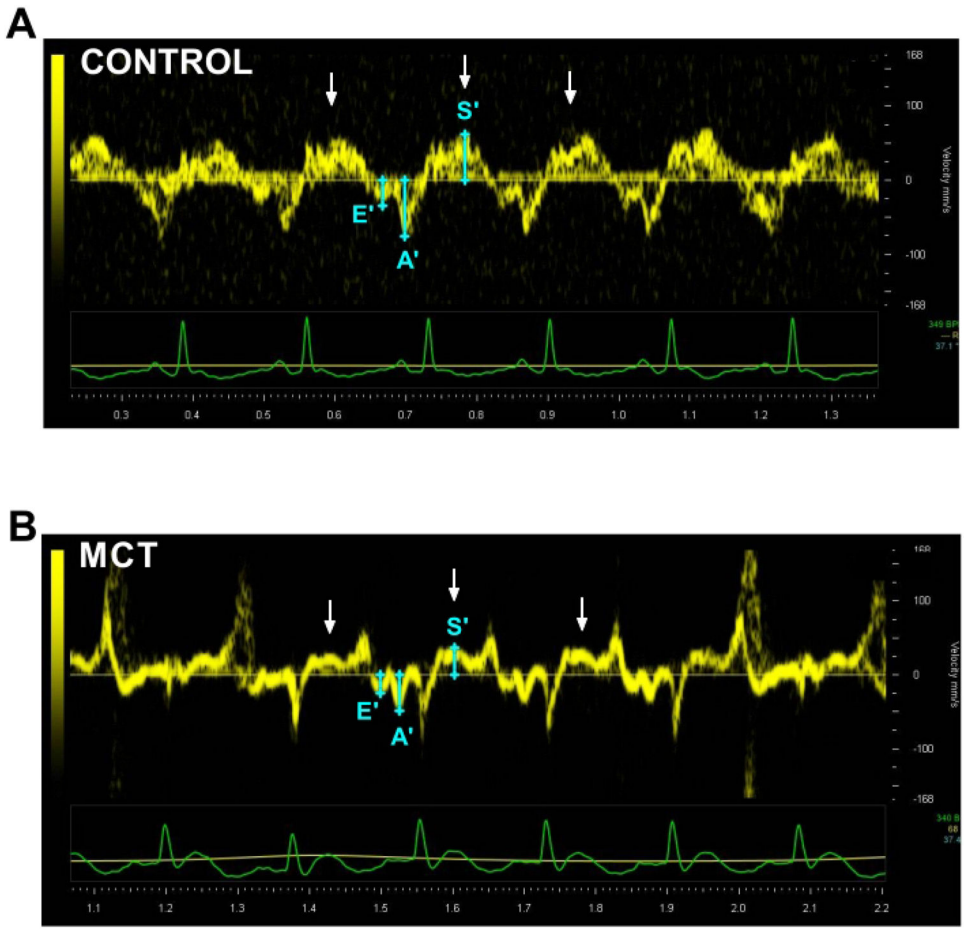


**Figure 6: Tissue Doppler of the lateral tricuspid annulus.**

Tissue Doppler sample images of peak systolic myocardial velocity at the lateral tricuspid annulus (S', in blue) and peak myocardial relaxation velocity at early diastole (E', in blue) and late diastole (A', in blue) in (**A**) a control rat and in (**B**) a monocrotaline (MCT)-treated rat. Arrows indicate the three consecutive cycles that were considered for calculations. Representative measurements are shown in one cycle for easy viewing, but all measurements were taken in each of the three cycles.

*J Vis Exp*. Author manuscript; available in PMC 2023 July 20.

**Table 1:**

**Right ventricle echocardiographic parameters at Day 24 post-MCT (MCT Group) or vehicle (Control Group) administration in Sprague Dawley rats.**

Data presented as mean ± SD. Student's t-test was used to analyze data. *$p < 0.05$. Abbreviations: Monocrotaline (MCT), RV internal diameter during diastole (RVIDd), RV internal diameter during systole (RVIDs), RV free wall thickness (RVFWT), right atrial area (RAA), right ventricle end-diastolic area (RVEDA), right ventricular end-systolic area (RVESA), RV fractional area change (RVFAC), pulmonary ejection time (PET), pulmonary acceleration time (PAT), pulmonary peak systolic velocity (PV PSV), cardiac output (PV CO), stroke volume (PV SV), heart rate (HR), cardiac cycle length (CL), tricuspid annular plane systolic excursion (TAPSE), ejection time (ET), tricuspid closure open time (TCO), RV myocardial performance index (RVMPI), tricuspid annular velocity at systole (S'), velocity of blood flow across the TV during early diastolic filling (E), and tricuspid annular velocity at early diastole (E').

| Echocardiographic parameters | | Experimental groups | | | |
|---|---|---|---|---|---|
| | | Control (vehicle) | | MCT (60 mg/kg) | |
| | | mean ± SD | n | mean ± SD | n |
| Boby weight range (kg) | | 0.352-0.431 | 8 | 0.231-0.296 | 9 |
| Morphology | RVIDd (mm) | 2.72 ± 0.43 | 8 | 5.04 ± 1.68* | 9 |
| | RVIDs (mm) | 1.77 ± 0.52 | 8 | 4.04 ± 1.58* | 9 |
| | RVFWT (mm) | 0.59 ± 0.13 | 8 | 1.38 ± 0.30* | 9 |
| | PV diameter (mm) | 3.72 ± 0.38 | 8 | 3.50 ± 0.24 | 9 |
| | RAA ($mm^2$) | 17.97 ± 3.14 | 5 | 34.46 ± 12.15* | 8 |
| | RVEDA ($mm^2$) | 37.97 ± 6.57 | 5 | 52.78 ± 7.41* | 8 |
| | RVESA ($mm^2$) | 21.68 ± 8.41 | 5 | 44.40 ± 5.04* | 8 |
| Systolic function | RVFAC (%) | 44.16 ± 16.55 | 5 | 15.49 ± 5.07* | 8 |
| | PET (ms) | 70.78 ± 5.89 | 8 | 74.52 ± 7.65 | 9 |
| | PAT (ms) | 32.56 ± 6.01 | 8 | 20.23 ± 4.21* | 9 |
| | PAT/PET Ratio | 0.46 ± 0.10 | 8 | 0.27 ± 0.05* | 9 |
| | PV PSV (mm/s) | 1032.35 ± 100.76 | 8 | 605.85 ± 170.29* | 9 |
| | PVCO (mL/min) | 179.03 ± 39.92 | 8 | 73.04 ± 36.57* | 9 |
| | PVSV (µL) | 505.53 ± 114.04 | 8 | 215.97 ± 99.58* | 9 |
| | HR (bpm) | 358.52 ± 43.14 | 8 | 324.69 ± 42.35 | 9 |
| | CL (ms) | 169.86 ± 22.60 | 8 | 185.84 ± 22.56 | 9 |

| Echocardiographic parameters | | Experimental groups | | | |
|---|---|---|---|---|---|
| | | Control (vehicle) | | MCT (60 mg/kg) | |
| | | mean ± SD | n | mean ± SD | n |
| | PAT/CL Ratio | 0.20 ± 0.05 | 8 | 0.11 ± 0.02* | 9 |
| | TAPSE (mm) | 3.33 ± 0.63 | 7 | 1.47 ± 0.49* | 8 |
| | ET (ms) | 77.83 ± 11.16 | 7 | 78.52 ± 7.82 | 8 |
| | TCO (ms) | 92.93 ± 9.58 | 7 | 107.96 ± 11.77* | 8 |
| | RVMPI | 0.20 ± 0.09 | 7 | 0.39 ± 0.19* | 8 |
| | S' (mm/s) | 62.62 ± 12.78 | 6 | 25.90 ± 8.26* | 7 |
| Diastolic function | E (mm/s) | 460.33 ± 82.90 | 7 | 684.89 ± 177.53* | 8 |
| | E' (mm/s) | 53.07 ± 26.35 | 6 | 40.82 ± 23.34 | 7 |
| | E/E' | 9.79 ± 3.18 | 6 | 23.79 ± 17.34 | 7 |

**Table 2:**

**Organ measurements at Day 24 post-MCT (MCT Group) or vehicle (Control Group) administration in Sprague Dawley rats.**

Data presented as mean ± SD. Student's t-test was used to analyze data. *$p < 0.05$. Abbreviations Monocrotaline (MCT), heart weight (HW), lung weight (LW), right ventricle (RV), left ventricle (LV), and tibia length (TL).

| Necropsy parameters | Experimental groups | |
|---|---|---|
| | Control (Vehicle, n = 6-8) | MCT (60 mg/kg, n = 7-9) |
| HW/TL (mg/mm) | 29.4 ± 2.40 | 30.8 ± 3.22 |
| LW/TL (mg/mm) | 40.3 ± 2.03 | 55.8 ± 6.75* |
| (LV+S)/TL (mg/mm) | 20.6 ± 1.81 | 16.1 ± 1.00* |
| RV/TL (mg/mm) | 5.76 ± 0.53 | 10.6 ± 2.39* |
| RV/(LV+S) | 0.28 ± 0.03 | 0.66 ± 0.16* |
| TL (mm) | 39.3 ± 1.03 | 38.7 ± 1.74 |

## Materials

| Name | Company | Catalog Number | Comments |
|---|---|---|---|
| 0.9% sodium cloride injection USP | Baxter | 2B1324 | |
| Braided cotton rolls | 4MD Medical Solutions | RIHD201205 | |
| Depilating agent | Wallgreens | Nair Hair Remover | |
| Electrode gel | Parker Laboratories | 15-60 | |
| High frequency ultrasound image system and imaging station | FUJIFILM VisualSonics, Inc. | Vevo 2100 | |
| Isoflurane | MedVet | RXISO-250 | |
| Male sprague Dawley rats | Charles River Laboratories | CD 001 | CD IGS Rats (Crl:CD(SD)) |
| Monocrotaline (MCT) | Sigma-Aldrich | C2401 | |
| Rectal temperature probe | Physitemp | RET-3 | |
| Sealed induction chambers | Scivena Scientific | RES644 | 3 L size |
| Solid-state array ultrasound transducer | FUJIFILM VisualSonics, Inc. | Vevo MicroScan transducer MS250S | |
| Stainless steel digital calipers | VWR Digital Calipers | 62379-531 | |
| Ultrasound gel | Parker Laboratories | 11-08 | |
| Vevo Lab software | FUJIFILM VisualSonics, Inc. | | Verison 5.5.1 |